NRIAG JOURNAL OF ASTRONOMY AND GEOPHYSICS
2020, VOL. 9, NO. 1, 598–612
https://doi.org/10.1080/20909977.2020.1831305

Prediction of aquifer properties from vertical electrical sounding data using artificial neural network: case study of Ibadan Metropolis, South-western Nigeria

M. A. Oladunjoye[a], M. A. Adeniran[a], A. U. Chukwu[b] and A. O. Oyerinde[c]

[a]Department of Geology, University of Ibadan, Ibadan, Nigeria; [b]Department of Statistics, University of Ibadan, Ibadan, Nigeria; [c]Department of Geology, The Polytechnic, Ibadan, Ibadan, Nigeria

ABSTRACT

Adequate estimates of aquifer properties are of utmost importance for proper management of groundwater resources. In an effort to provide alternative way of estimating aquifer properties at minimum cost, Artificial Neural Network (ANN) model was generated for the prediction of Transmissivity (T) and Hydraulic Conductivity (K). Six hundred and thirty eight vertical electrical soundings data were acquired and interpreted to obtain Dar-Zarrouk parameters. The diagnostic relationship between the K values measured in reference wells and electrical soundings data was combined with Dar-Zarrouk parameters to estimate T and K. Transverse resistance (R), thickness (h), resistivity (ρ), K and T were subjected to ANN analysis using SPSS software and Python. The results showed that R ranges from 40 to 21552 Ωm2, h ranges from 1.4 to 40.0 m, ρ ranges from 4 to 754 Ωm. K varies from 0.004 to 0.800 m/day and T varies from 0.04 to 18.20 m2/day within the study area. ANN model was able to predict K and T values with an accuracy ranging from 97 to 99%. RMSE values for the prediction ranged from 0.063 to 0.250. The ANN model generated was able to predict K and T of the aquifer from geo-electrical data at minimum cost.

ARTICLE HISTORY
Received 9 May 2020
Revised 24 August 2020
Accepted 29 August 2020

KEYWORDS
Vertical electrical sounding; aquifer; transmissivity; hydraulic conductivity; artificial neural network; prediction

1. Introduction

Groundwater is believed to be the only viable source of water in many areas where the development of surface water supply for physical/industrial development to achieve maximum human growth is not well developed. Groundwater is an important source of water for drinking, irrigation, and industrial uses. It is also a major source of domestic water requirement. The provision of water for domestic and other uses in both rural and urban centres is one of the most intractable problems in Nigeria today. In order to solve this problem, it is important to investigate the properties that influence the availability of groundwater. Hydrogeological and geophysical methods has proven to be an effective tool in estimating aquifer parameters.

In-situ hydrogeological measurement can be carried out through pumping test, grain size analysis, and tracer techniques from which subsurface parameters such as transmissivity, hydraulic conductivity, storativity, etc., can be obtained in an aquifer (Sanuade et al. 2018). This approach tends to be expensive and take a longer time to execute. Geophysical methods have also been used in estimating the physical properties of the subsurface. These physical properties have a direct relationship with the aquifer properties that govern the occurrence and flow of groundwater. However,modelling strategies have been recognised as the most important tool for resolving environmental issues such as management of non-point source emissions, conservation of source water, and management of nutrients. There is currently a trend towards physically-based models in which saturated hydraulic conductivity is the most significant parameter. The saturated hydraulic conductivity has also been identified as a highly spatially variable hydraulic property and the simulation process requires an estimate of the representative values of this parameter for each watershed area or sub-basin.

Various geophysical and hydrogeological parameters have established relationships that are made possible by the correlation that exists between the physical measurements obtained from the two approaches. There is, for example, a relationship between electrical resistivity (ρ) and transmissivity (T) which is as a result of the linkage of both parameters to pore space structure and heterogeneity (Soupios et al. 2007). Generally, geophysical methods are cost-effective, non-destructive and fast to implement as compare to direct in-situ measurements. In order to understand the relationship that exists between geophysical and hydrogeological parameters, several experiments were carried out by researchers by taking into account the physical laws that are associated with subsurface processes (Niwas and Singhal

CONTACT M. A. Adeniran adeniranmargaret93@gmail.com Department of Geology, University of Ibadan, Ibadan, Nigeria

1981; Niwas and Lima 2003). Ahmed et al. (1988) have explored the connections between transverse resistance and transmissivity by using a geo-statistical approach. Youssef (2020) employed a geo-statistical approach in interpreting Dar-Zarrouk parameters estimated for surface electrical measurement, from which he generated the spatial distribution properties of electric anisotropy, aquifer hydraulic characteristics and groundwater quality. Sanuade et al. (2018) implement the application of a nonlinear artificial neural network model to estimate transmissivity in a basement complex environment.

Furthermore, Artificial Neural Networks (ANNs); a type of non-linear regression computational tools (Basheer and Hajmeer 2000) whose application in predicting aquifer properties from surface geophysical measurement have not been fully explored. According to Hornik et al. (1989), the theoretical implementation of multilayer feed-forward networks as universal approximators has been proven.

Most attempts of using ANNs for prediction of hydraulic conductivity (K) often use its relationship with particle size, i.e., clay, silt, and sand as input (Bart et al. 2016; Al-Sulaiman and Aboukarima 2016). Little work has been done as regards the implementation of applicability of electrical resistivity due to data scarcity and limited accessibility. In addition, it is of utmost importance to quantify the degree of uncertainty in stochastic modelling associated with the predictions. One of the key features of ANNs is that it has the ability to identify hidden patterns in large data sets, which provides an ideal way for characterising the heterogeneity of basement complex terrains.

Most of the previous studies use correlation and geo-statistical analysis to characterise the relationship that exists between hydrogeological and geophysical parameters. The main objective of this research is therefore to establish an Artificial Neural Network (ANN) ensemble modelling approach to aquifer properties on three different rock types, thereby enabling its applicability on other areas with similar geology. The novel attributes of ANN is that it is information driven, which gives an exceptional means of predicting both transmissivity and hydraulic conductivity.

1.1. Geological settings

The study area is located between Latitudes 7°17′00” to 7°31′00” North of the Equator and Longitudes 3° 46′00” to 3°59′00” East of the Greenwich Meridian, covering about 540 km^2 (Figure 1). The city has a population of about 3.6 million according to the 2006 population estimate. Accessibility of the area can be best described in terms of its road network. The city is readily accessible by roads. The study area is relatively rugged with undulating topography. According to Jones and Hockey (1964), the relief of the basement complex is closely associated with the underlying rocks. The elevation varies between 160 and 360 m above mean sea level with an average of 230 m. The study area is well-drained by rivers and streams that are topographically controlled and flow in

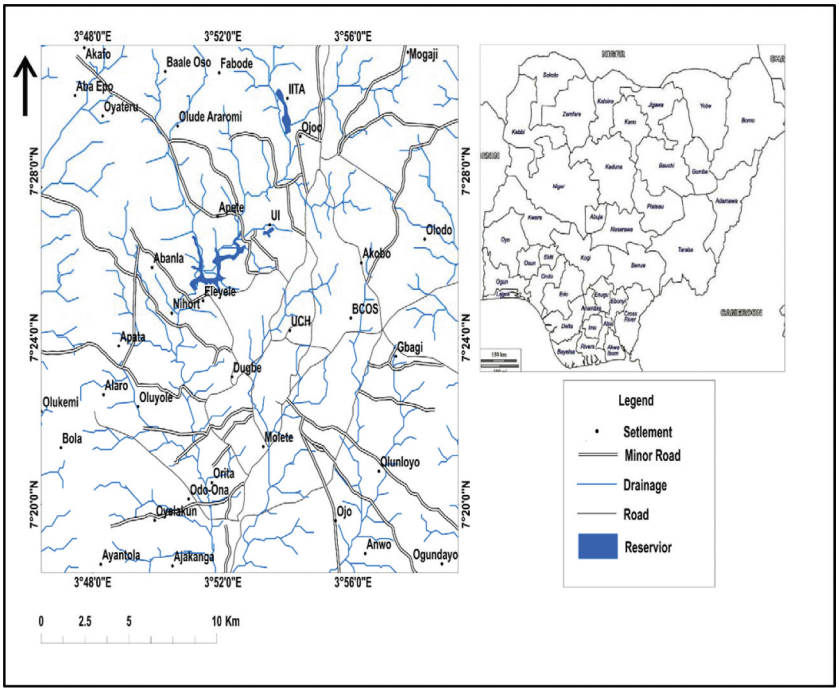

Figure 1. Topographic map of Ibadan showing the study area.

the direction of rock strike. The dominant rock types in Ibadan area are the quartzite of the metasedimentary series, migmatite – gneiss complex comprising the banded gneiss, augen gneiss and the migmatite (Figure 2). These rocks are intruded by pegmatite, quartz veins, aplites and dolerite dykes (Oladunjoye and Jekayinfa, 2015). Quartz schist outcrops occur as long ridges with relative a high elevation and strike running in the N – S direction between 340° and 350° with a consistent eastern dip. The western and eastern part of the study area is covered by Migmatite gneiss complex with N – S strike direction and with an average dip angle of 47° W and 36° E. In some places, they are obliterated by intrusive veins and dykes. Minor structures like folds, shear zones, pinch and swell structures, concordant and discordant quartz veins and quartz are present on the migmatite gneiss complex.

The trends of foliation and joints in the rocks largely controls the direction of the rivers, imposing a dendritic pattern on the drainage with irregular branching of tributary streams (Figure 3). Major rivers that drain the area include river Omi, Ona, Ogunpa and Kudeti which are fed by steams from different parts of the city.

2. Materials and methods

Three major methods were employed in carrying out the investigation for the prediction of aquifer properties within the study area. These are geophysical investigation, hydrogeological investigation (pumping test) and Statistical modelling. Figure 4 shows the step by step implementation of the methods used.

2.1. Geophysical investigation

Geophysical investigation involving vertical electrical sounding was employed for this research. Six hundred and thirty eight vertical electrical sounding data were acquired using Schlumberger array technique with maximum current electrode separation of 133 m and maximum potential spacing of 10 m. The Vertical Electrical Sounding points were distributed over three different rock types (Figure 5) – Migmatite Gneiss,

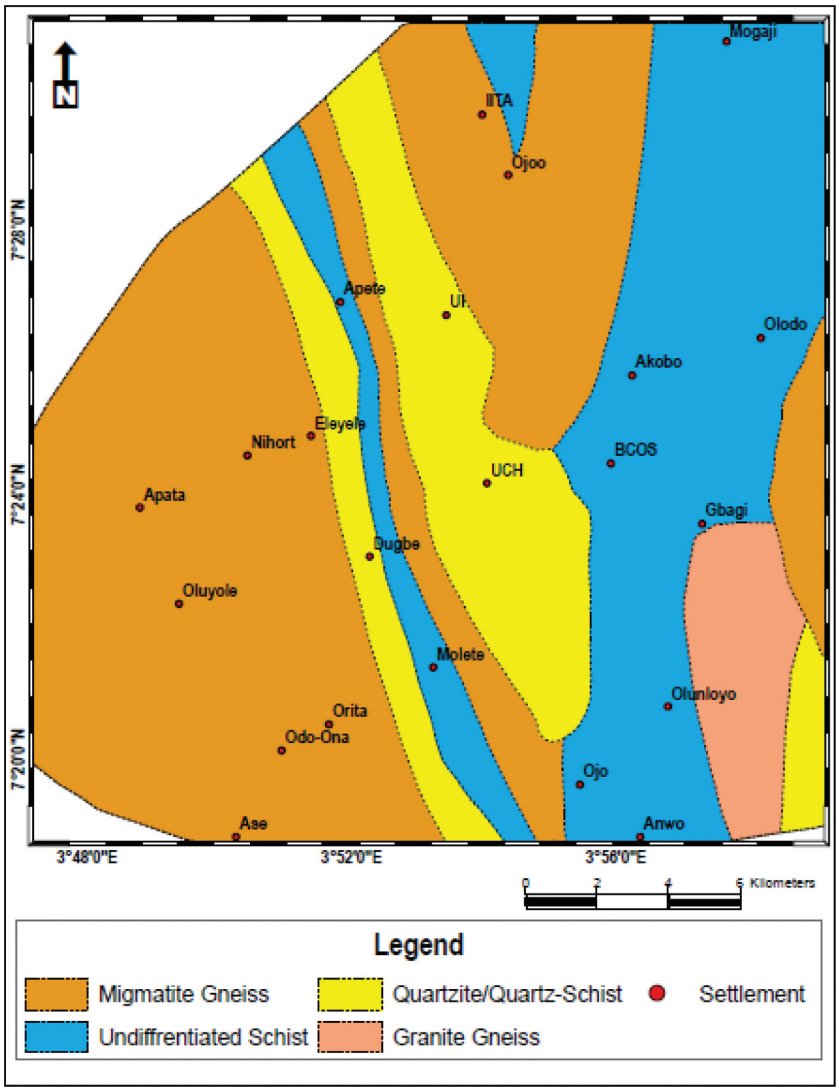

Figure 2. Geological map of the study area (Modified after Oladunjoye and Jekayinfa 2015).

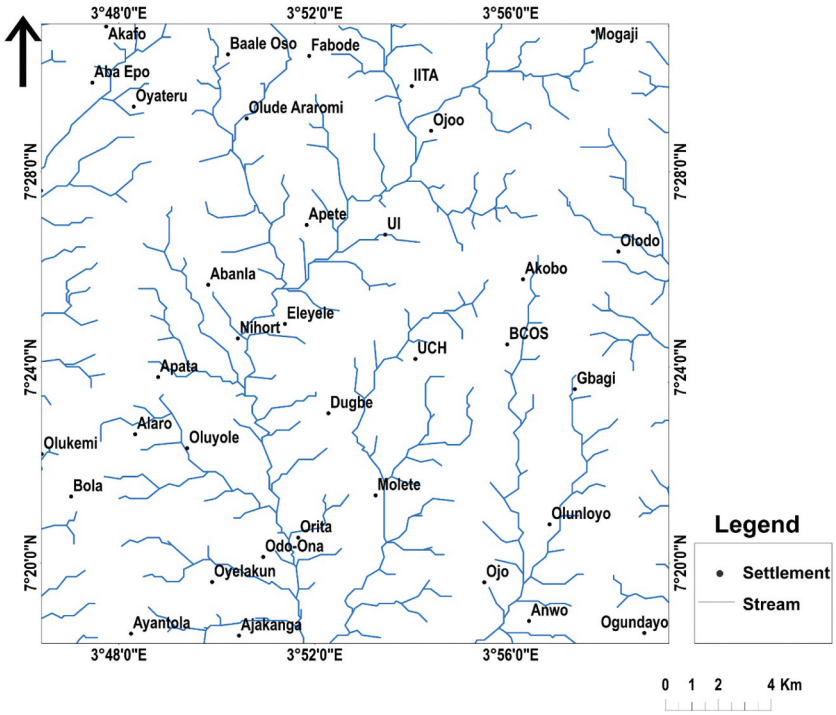

Figure 3. Drainage map of the study area.

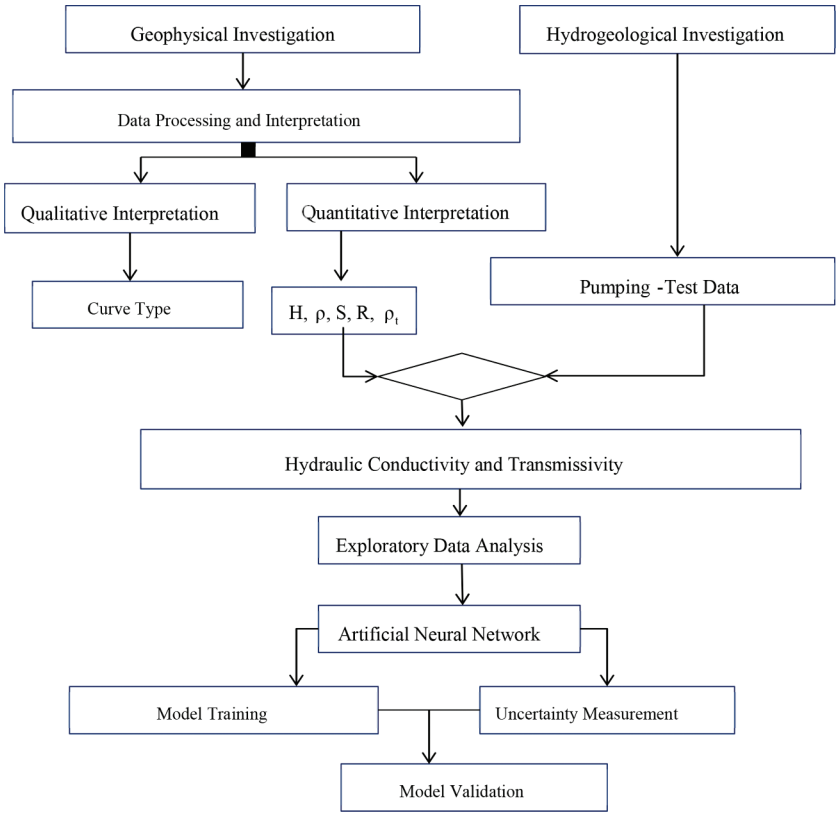

Figure 4. Flow chart showing the methods adopted for the study.

Undifferentiated Schist and Quartzite/quartz-schist, with Migmatite having 50% (323 points) of the data set, Undifferentiated schist 33% (208 data points) and Quartzite/quartz-schist 17% (107 data points). The obtained VES data were interpreted using partial curve matching technique and computer iteration program (WINRESIST), which enables accurate estimation of the layer parameters (layer resistivities and thicknesses).

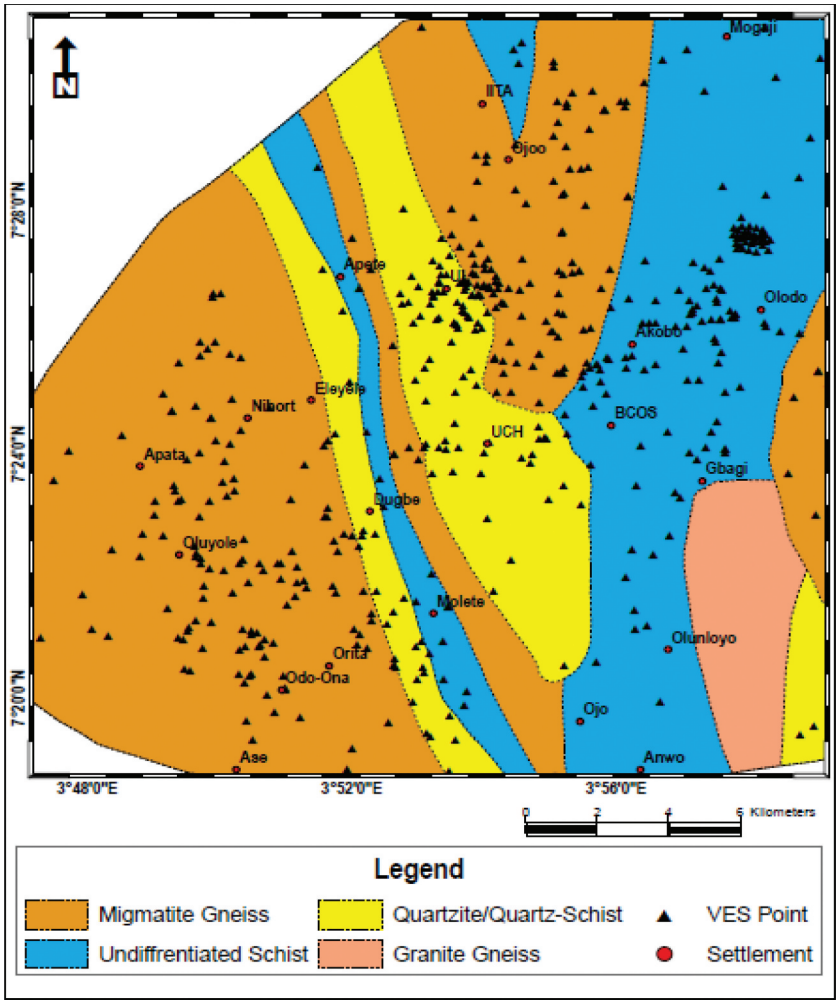

Figure 5. Geological map of the study area showing distribution of VES points.

2.2. Hydrogeological investigation

Pumping test results obtained by Tijani et al. (2009) and (2018)) on the Migmatite Gneiss, Quartzite/Quartz-Schist and Undifferentiated Schist was used in this research. The pumping test operation involved the pumping out of groundwater from drilled boreholes and measuring the response of the aquifer in terms of water level, discharge rate and pumping duration, before and after pumping. The obtained data were analysed using the straight line method, where drawn down was plotted with an arithmetic scale on the y-axis against the logarithm time scale on the x-axis.

2.3. Estimation of Dar-Zarrouk parameters and aquifer parameters

The layered parameters obtained from the VES were used to compute the Dar-Zarrouk parameters which include transverse resistance, transverse resistivity, longitudinal resistivity (aquifer resistivity), and longitudinal conductance (Maillet 1947). The equations used in obtaining these parameters are listed below.

Aquifer Thickness (h_a)

$$h_a = \sum^{h_i} \tag{1}$$

Aquifer Resistivity (ρ_a)

$$(\rho_a) = \rho_{L=\frac{ha}{S}} = \frac{\sum^{h_i}}{\sum^{\frac{h_i}{\rho_i}}} \tag{2}$$

Longitudinal Conductance (S):

$$S = n\sum_{i=1}\left[\frac{h_i}{\rho_i}\right], S = \frac{h_1}{\rho_1} + \frac{h_2}{\rho_2} + \frac{h_3}{\rho_3} + \ldots + \frac{h_n}{\rho_n}\left(\Omega^{-1}\right) \tag{3}$$

Transverse Resistance (R)

$$R = h_1\rho_1 + h_2\rho_2 + h_3\rho_3 + \ldots + h_n\rho_n\left(\Omega m^2\right) \tag{4}$$

Transverse Resistivity (ρ_t):

$$\rho_t = \frac{R}{h} = \frac{\sum^{h_i}\rho_i}{\sum^{h_i}}() \tag{5}$$

Longitudinal Resistivity:

$$\rho_t = \frac{R}{h} = \frac{\sum^{h_i}\rho_i}{\sum^{h_i}}() \tag{6}$$

Transmissivity (T); the product of hydraulic conductivity and aquifer thickness, can be derived in term of R and S as

$$T = K\sigma R \tag{7}$$

And

$$T = \left(\frac{K}{\sigma}\right)S \tag{8}$$

It has been observed by Niwas and Singhal (1981) that either of the two proposition. Kσ = constant or K/σ = constant be true for an area under study, also valid for other areas with similar geological setting and water quality. Hence, knowing the hydraulic conductivity (K) values of existing boreholes via pumping test and electrical conductivity (σ) values of the aquifer extracted from the geo-electric data carried out at the borehole location, it is possible to determine the transmissivity values and its variation from place to place even for areas without boreholes (Niwas and Singhal 1981)

Since

$$K_{PT}\sigma = Constant(A) \tag{9}$$

Then

$$K_{call} = \frac{A}{\sigma} \tag{10}$$

$$T_{cal} = K_{cal}\sigma R \tag{11}$$

Where;

$$\mathrm{A} = \mathrm{Constant}\left(\frac{Siemen}{day}\right)$$

K_{PT} = Hydraulic conductivity from pumping test

K_{cal} = Calculated hydraulic conductivity (m/day) at each VES point

T_{cal} = Calculated transmissivity (m^2/day) at each VES point

2.4. Artificial Neural Network (ANN)

According to Singh et al. (2013), ANN is a form of artificial intelligence that imitates the human brain by gaining knowledge through a learning process. ANN can model non-linear problems without implicit functions as it is in the case with the traditional statistical approaches. In this research, a supervised feed-forward multilayered perception network was used for the estimation of K and T. The ANN network consists of an input layer, a hidden layer and an output layer. The independent variables, i.e., the predictors are fed into input layer neurons of the network. Weight values are then attached to each of these predictors, after which they are being transferred into the hidden layer neurons. A hidden-layer neuron sum the weighted value obtained from each input neuron, along with a bias, and then transfer it as a non-linear transfer function on to the output. The neurons of the output serve the same function as a hidden neuron.

The sets of input and output variables were used in training the network. The target output at each output neuron was achieved by gradual adjustment of the weights and the associated biases values. ANN training structure consists of the weights between the neurons, a transfer function and a learning algorithm. The weights determine the importance of each input variable while the transfer function serves as a control for the outputs generated from each of the neurons. At the beginning of each training process, each input neuron receives a prearranged weight values to its variable and combines these weighted inputs. Mathematically, the combined weight input is given by:

$$net_j = \sum^{x_i} v_{ij} - b_j \tag{12}$$

net_j: summation of the weighted input for the j^{th} neuron; x_i is the input from the i^{th} neuron to the j^{th} neuron;

$\mathbf{v_{ij}}$: is the weight from the i^{th} neuron in the previous layer to the j^{th} neuron in the current layer;

$b_{j:}$ is the bias, associated with node j.

The neuron's bias must be exceeded in this network before it can be activated. The activation level is evaluated by passing the net_j value through a transfer function. An iterative process is employed for the execution of the training process such that the level of the strength of each activation function of a neuron brings about the transfer of output as an input to the adjacent neurons. The activation function used for the training phase is the sigmoid function which can be expressed as

$$f(net_j) = \frac{1}{1 + e^{-netj}} \tag{13}$$

The number of hidden layer neurons used was determined by the trial and error approach. At each stage of the study, the number of neurons was increased to maximise the ANN model. A typically back-propagation algorithm was employed in the learning phase of ANNs. Back-propagation in multi-layered feed-forward networks is the most widely used supervised training algorithm. In back-propagation networks, information from the input layer to the hidden layer and then to the output layer is transmitted in the forward direction. The ANN structure was used in constructing the model as shown in equations 9 and 10, and the structure of the model is also shown in Figure 6.

Hydraulic Conductivity =

$$\left[\sum_{i=1}^{N} w_{2i}\left(\frac{1}{1+e^{-2\left(w_{1i,1}(R)+w_{1i,2}(\rho)+b_{1i}\right)}}\right)\right]+b_2 \tag{14}$$

Transmissivity =

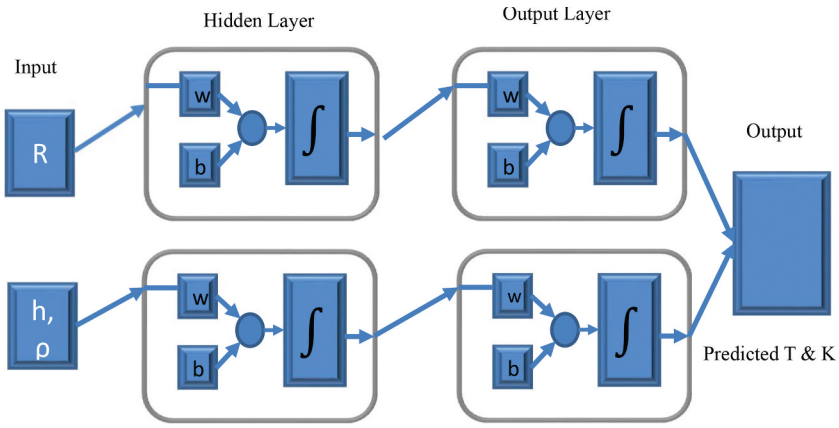

Figure 6. Artificial neural network architecture.

$$\left[\sum_{i=1}^{N} w_{2i}\left(\frac{1}{1+e^{-2\left(w_{1i,1}(R)+w_{1i,2}(h_a)+b_{1i}\right)}}\right)\right]+b_2 \qquad (15)$$

Where N is the total number of neurons, w_1 and w_2 are weights of the hidden layer and output layer, respectively, b_{1i} and b_2 are the bias of the hidden and the output layer, respectively, R is transverse resistance, h is the aquifer thickness and ρ is the aquifer resistivity.

3. Results and discussion

3.1. Geo-electric interpretation

The electrical resistivity data interpretation reveals a three to five subsurface geo-electric layers with a lithological sequence of topsoil, laterite/clay, weathered formation, fractured basement, and bedrock. The three-layer system confirms the occurrence of an aquiferous weathered layer or fractured saprolite zone sandwiched between more resistive topsoil and bedrock, a situation that is typical of the basement rock settings.

The distribution of the geo-electric parameters is shown in Figure 7 using a box-plot. The summary of the geo-electric parameter is presented in Table 1. Topsoil thickness varies between 0.2 and 4.2 m (mean: 1.05) in migmatite, 0.3–9 m (mean: 1.28) in undifferentiated schist and 0.2–3.6 m (mean: 1.15) in quartzite/quartz schist locality (Table 1). The topsoil resistivity values range from 20–1700 Ωm (mean: 277), 20–1169 Ωm (mean: 227) and 12–1143 Ωm (mean: 240) for migmatite, undifferentiated schist and quartzite/quartz schist, respectively. Weathered layer thickness values obtained ranged from 0.9 to 26 m (mean: 8.8), 0.4–37 m (mean: 10.5) and 1.3–44.8 (mean: 14.2) for migmatite, undifferentiated schist and quartzite/quartz schist, respectively. The weathered layer thickness was seen to be thickest within the quartzite/quartz schist lithology and this can be related to ease at which the rock weathered. The obtained weathered layer resistivity values vary between 10 and 979 Ωm (mean: 96), 6–881 Ωm (mean: 126) and 10–880 Ωm (mean: 136) for migmatite gneiss, undifferentiated schist and quartzite/quartz schist lithology. High resistivity value obtained within the quartzite/quartz schist lithology can be attributed to the quarzitic nature of the aquifer. Low resistivity value obtained from within migmatite lithology is as a result of the weathered zone been mostly dominated by clayey materials.

The basement resistivity values ranged from 12 to 6977 (mean: 879), 10 to 6988 Ωm (mean: 714) and 11 to 8128 Ωm (mean: 525) in migmatite gneiss, undifferentiated schist and quartzite/quartz schist lithology. Based on the resistivity values obtained, the degree of fracturing was more prominent in quartzite/quartz schist lithology with migmatite gneiss having the least degree of fracturing.

The aquifer thickness obtained from VES data varied between 1.6 and 37.5 m (mean: 11.3) in Migmatite Gneiss, 1.4–40.6 m (mean: 13.24) in undifferentiated schist and 3.1–57.1 m (mean: 18.26) in the quartzite/quartz schist lithology. Figures 8(a) and 9 show the aquifer thickness distribution within the three rock types and the spatial variation in aquifer thickness in the study area. From the result, the quartzite/quartz-schist and undifferentiated schist bedrock exhibit high aquifer thickness value, this was expected because of the easy of fracturing and deep weathering of the bedrock to give a thick overburden. However, low aquifer thickness value was obtained within the migmatite gneiss region which was due to the bedrock resistance to weathering. Greater depth to basement indicates larger space to accommodate the infiltrating water but the type of material occupying this space must be put into consideration when using the aquifer thickness to estimate the hydraulic potential of an area, as clayey materials are only known to be porous but not readily permeable to release water to the underlying fractured bedrock and the penetrating borehole.

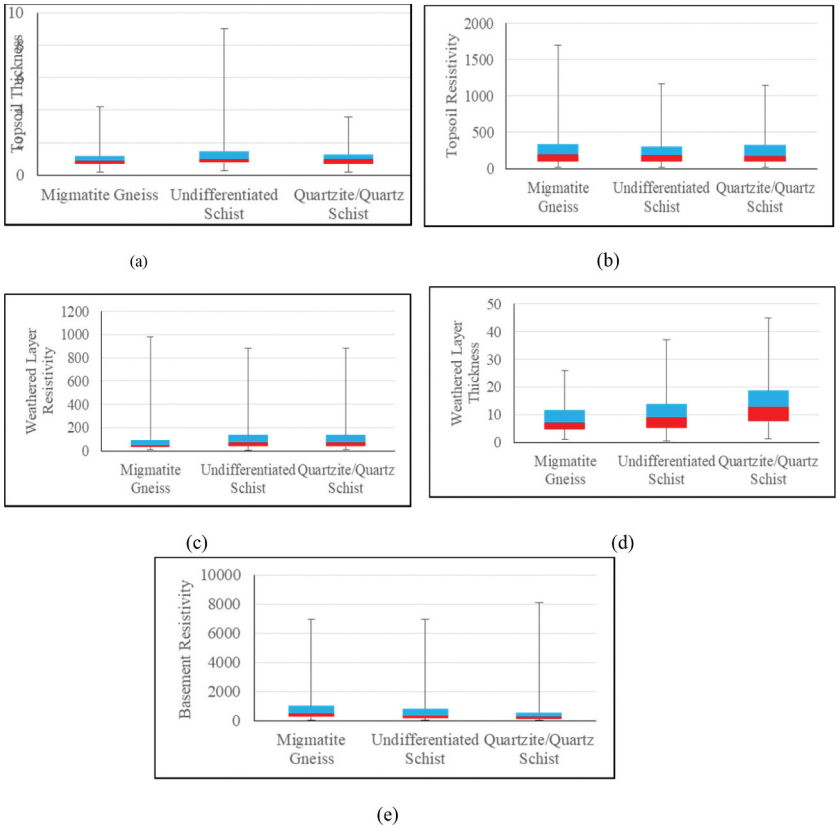

Figure 7. Box plot showing the distribution of (a) Topsoil thickness (b) Topsoil resistivity (c) Weathered layer resistivity (d) Weathered layer thickness (e) Basement resistivity, within migmatite gneiss, undifferentiated schist and quartzite/quartz schist lithology.

Table 1. Summary of geo-electric parameters and Dar-Zarrouk parameters.

	Migmatite Gneiss			Undiffrentiated Schist			Quartzite/Quartz Schist		
	Min.	Max.	Mean	Min.	Max.	Mean	Min.	Max.	Mean
Aquifer Thickness (m)	1.6	37.5	11.3	1.4	40.6	13.24	3.1	57.1	18.26
Aquifer Resistivtity (Ωm	9	671	77	7	754	112	4	542	101
Longitudinal Conductance (Ω^{-1})	0.01	1.92	0.23	0.01	1.52	0.22	0.32	1.60	0.32
Total Transverse Resistance (Ωm^2)	40	13,024	1429	97	13,573	1855	49	21,552	2525
Transvere Resistivity (Ωm)	11.01	824.34	115.11	13.9	784.32	137.89	15.93	751.62	133.9

Longitudinal Resistivity varies between 9 and 671 Ωm (mean: 77) in migmatite gneiss, 7–754 Ωm (mean: 112) in the undifferentiated schist and 4–542 Ωm (mean: 101) within quartzite/quartz schist. Longitudinal resistivity values were used as the aquifer resistivity due to the longitudinal characteristic of the understudy aquifer where the weathered layer (regolith) is underlain by more resistive fresh bedrock (Reiter 1981).

Figures 8(b) and 10 show the distribution and variation plot of the aquifer resistivity of the study area. From the plot, it could be observed that the high aquifer resistivity values occur mostly within the migmatite gneiss region, which is as a result of the materials that constitute the overburden. However, within the quartz/quartz schist and the undifferentiated schist region, there exists a relatively low aquifer resistivity which is an indication of weathering of schist to clay. The wide variation in this parameter indicates the inhomogeneity of the basement complex aquifers as indicated by Murali and Patangay (2006).

The transverse resistance values vary from 40 to 13,024 Ωm^2 (mean: 1429) within the Migmatite terrain, 97–13,573 Ωm^2 (mean: 1855) in the undifferentiated schist and 49–21,552 Ωm^2 (mean: 2525) within quartzite/quartz schist. Figure 11 represents a variation plot of the transverse resistance of the study area. The low values of transverse resistance observed within the quartzite/quartz-schist can be attributed to the presence of clayey materials which are only known to be porous but not readily permeable to release water to the underlying fractured bedrock. On a purely empirical basis, it can be admitted that transmissivity is directly proportional to the transverse resistance (Ungemach et al. 1969). Therefore, transverse resistance could be used in the

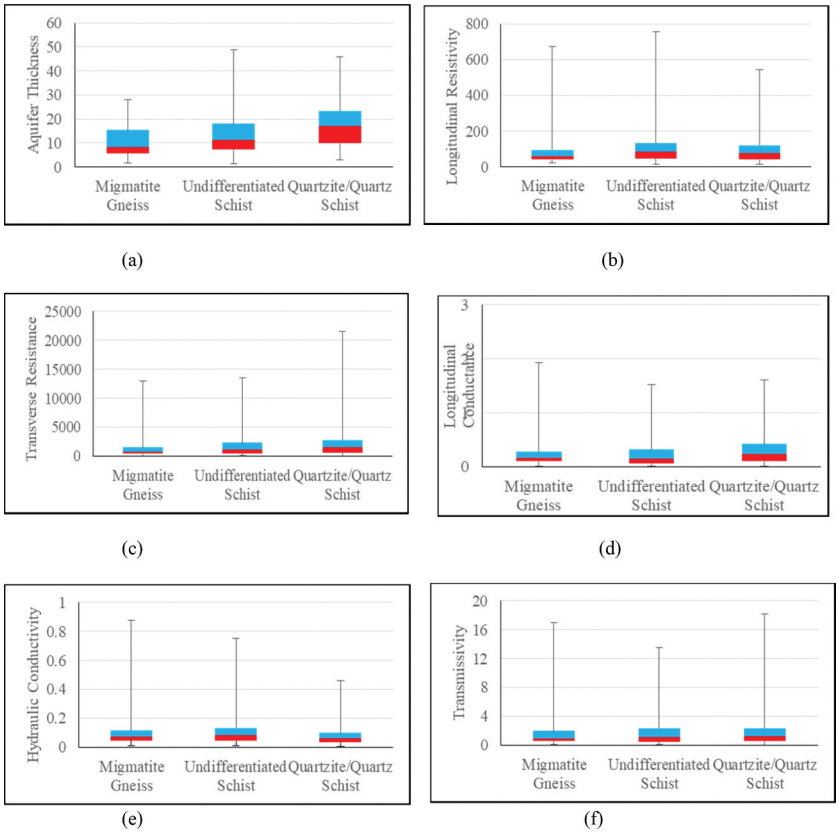

Figure 8. Box plot showing the distribution of (a) Aquifer thickness (b) longitudinal resistivity (c) Transverse resistance (d) Longitudinal conductance (e) Hydraulic conductivity (f) Transmissivity, within migmatite gneiss, undifferentiated schist and quartzite/quartz schist lithology.

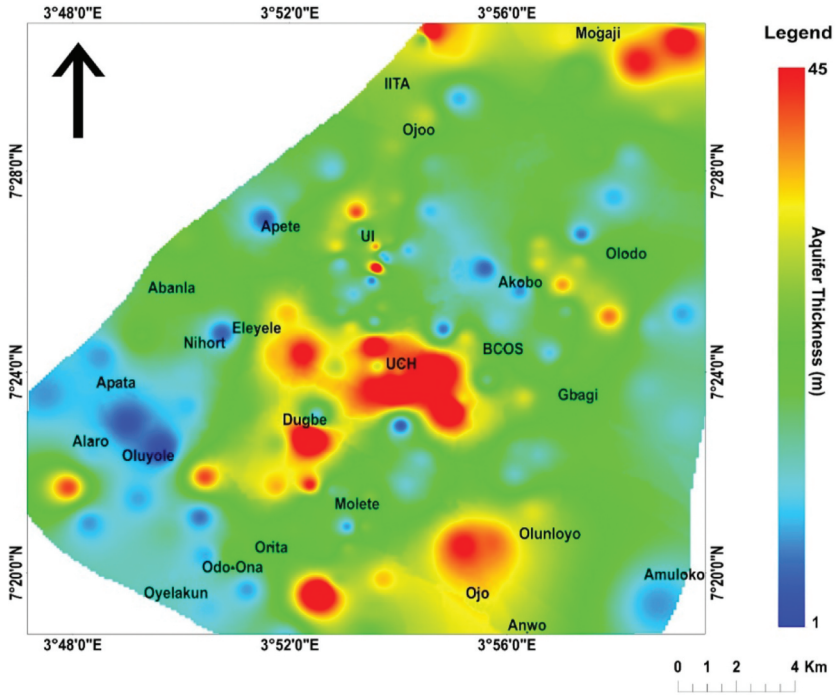

Figure 9. Spatial distribution of aquifer thickness within the study area.

determination of zones with high groundwater potential suitable for drilling wells.

The values of hydraulic conductivity (K) estimated from geo-electric data varies from 0.01 to 0.87 m/day (mean: 0.1), 0.007–0.75 m/day (mean: 0.11) and 0.004 –0.457 m/day (mean: 0.085) in migmatite, undifferentiated schist and quartzite/quartz schist. Figure 12 shows the spatial

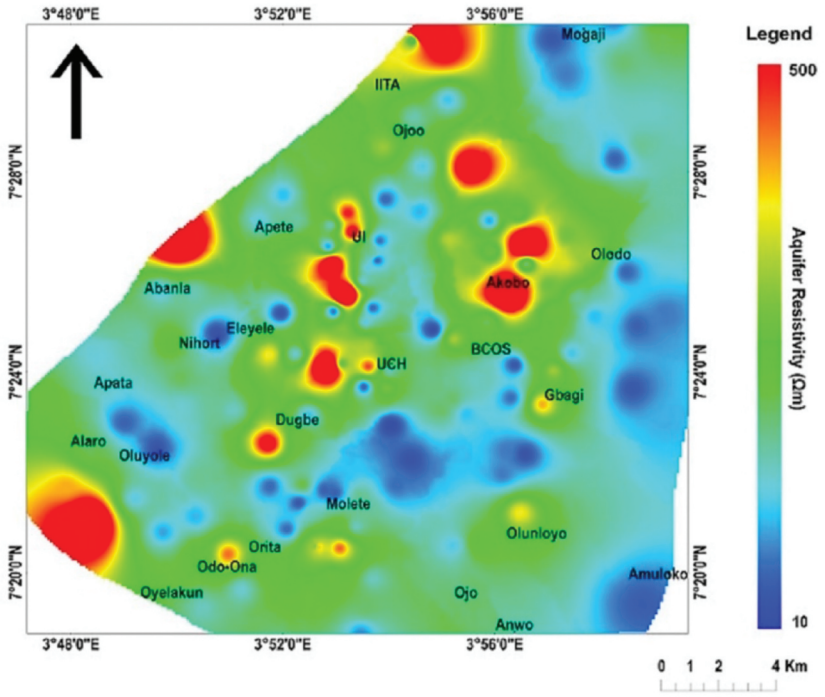

Figure 10. Spatial distribution of aquifer resitivity within the study area.

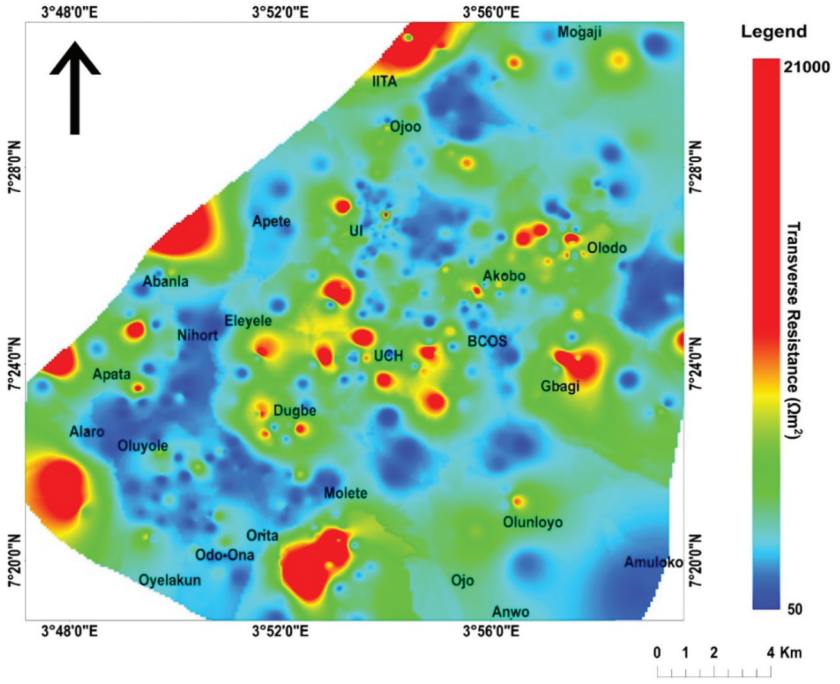

Figure 11. Spatial distribution of transverse resistance within the study area.

distribution of hydraulic conductivity within the study area. The low values observed within the Quartzite/Quartz Schist can be attributed to high clay content thereby making restricting the ease at which water is being released from the underlying-fractured bedrock. This value falls within the range of minimum and maximum value for the weathered igneous and metamorphic rocks (0.015244–3.04878 m/day) as given by **Halford and Kuniasky (2002)**. Also, the values fall within the range of the hydraulic conductivity determined by **Tijani et al. (2009)**. Table 2 shows a summary of the hydraulic properties obtained from the study area.

The calculated transmissivity values varies from 0.03 to 16.98 m^2/day (mean: 1.86), 0.097–13.53 m^2/day (mean: 1.78) and 0.04–18.1 m^2/day (mean: 2.13) in migmatite, undifferentiated schist and

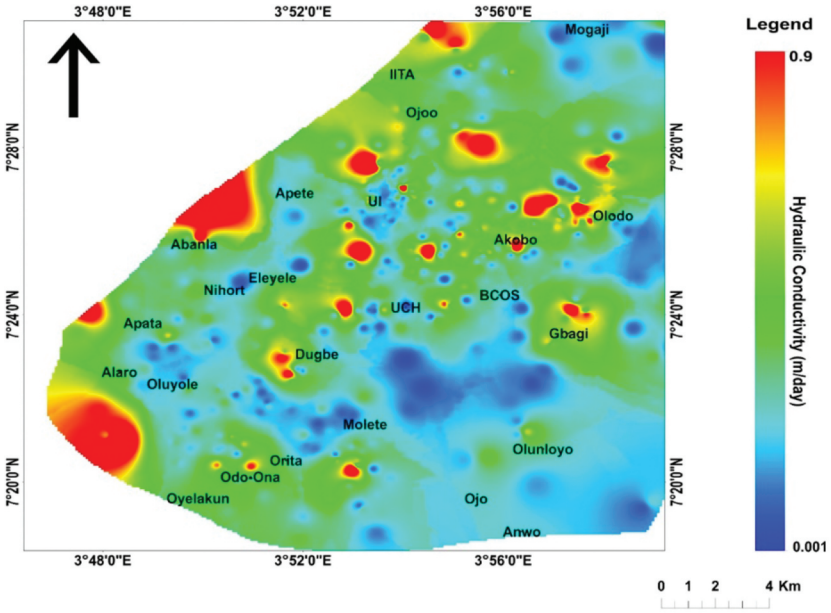

Figure 12. Spatial distribution of hydraulic conductivity within the study area.

Table 2. Summary of hydraulic properties values obtained within the study area.

	Migmatite Gneiss			Undiffrentiated Schist			Quartzite/Quartz Schist		
	Min.	Max.	Mean	Min.	Max.	Mean	Min.	Max.	Mean
Hydraulic Conductivity (m/day)	0.01	0.87	0.1	0.007	0.75	0.11	0.004	0.457	0.085
Transmissivity (m^2/day)	0.03	16.98	1.86	0.097	13.53	1.78	0.04	18.1	2.13

quartzite/quartz-schist, respectively. Low T values (<1–5 m^2/day) are characteristic of the basement aquifer, except when there is a highly transmissive-fractured zone (Nur and Goji 2005). Figure 13 shows the spatial distribution of transmissivity within the study area.

3.2. Validation and correlation with pumping test results

Tijani et al. (2009), (2018)) conducted a total of twenty-two (22) pumping test within the study area. The pumping test was analysed to determine the impacts of the underlying bedrock types on the

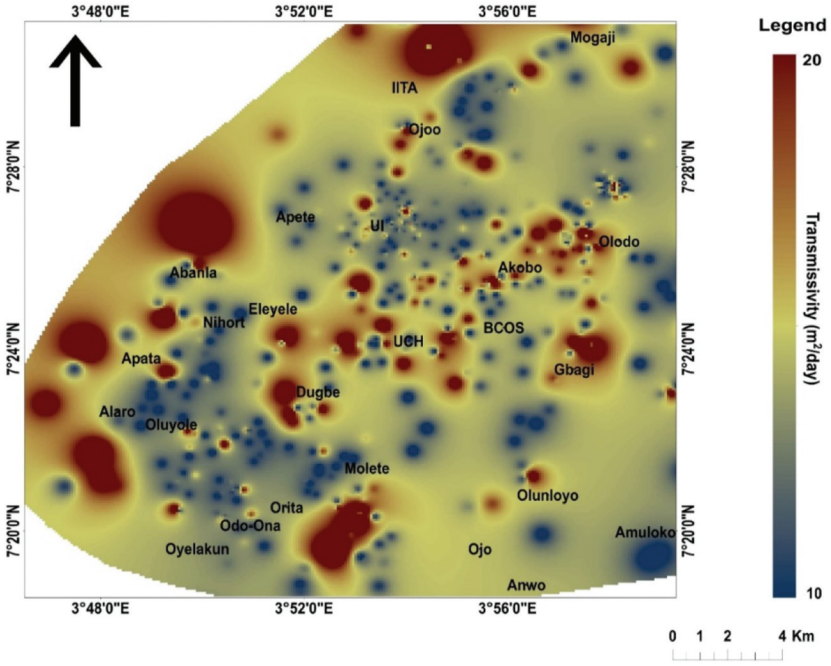

Figure 13. Spatial distribution of transmissivity within the study area.

hydraulic characteristics. The borehole data revealed average saturated thickness which varies from 30 m in Migmatite to 62.6 m in Quartzite/Quartz Schist and 22 m in Undifferentiated Schist. The observed yield was generally low with an average value of about 80.8 m^3/day in all the three bedrock settings.

The estimated transmissivity (T) ranges from 1.1 to 4.2 m^2/day (mean, 2.8 m^2/day) in Migmatite, 3.63–4.62 m^2/day(mean, 4.1 m^2/day) in Undiffrentiated Schist and 0.41–10.6 m^2/day (mean, 2.7 m^2/day) in the quartzite/quartz Schist environment. The estimated hydraulic conductivity values vary between 0.001 and 0.14 m/day (mean 0.075 m/day) in Migmatite, 0.17–0.21 m/day (mean, 0.19) in Undifrentiated Schist and 0.01–0.18 m/day (mean 0.046 m/day) in Quartzite/Quartz Schist.

3.3. Relationships between hydro-geological and hydro-geophysical estimated hydraulic properties

The hydraulic properties estimated using geophysical method and those determined via pumping test were correlated. The hydro-geophysical and hydro-geologically estimated hydraulic properties obtained in this study showed a good positive correlation of 0.82 to 0.99 for hydraulic conductivity and transmissivity, respectively (Figures 14 and 15). This correlation is a good indication of the applicability of geophysical method in the determination of hydraulic parameters. This is consistent with previous works of Giansilvio et al. (1984) and Kumar et al. (2001).

3.4. Artificial neural network

The regression model used for the implementation of the ANN model is displayed in Figure 6. Figures 16, 17 and 18 display the scattered plot of the output generated during the training phase. The coefficient of correlation for the training result are 0.99, 0.99 and 0.99 for transmissivity and 0.98, 0.99, and 0.97 for hydraulic conductivity for quartzite/quartz schist, undifferentiated schist and migmatite gneiss, respectively. Figures 19, 20 and 21 show the scattered plot of testing data used in validating the model, with a correlation coefficient of 0.99, 0.99 and 0.98 for transmissivity and 0.99, 0.98, and 0.98 for hydraulic conductivity for quartzite/quartz schist, undifferentiated schist and migmatite gneiss, respectively. There is some variation from the expected values between the predicted values of K and T. The variance, however, is within an acceptable limit of less than 5% (Sanuade et al. 2018).

In order to test the efficacy of the predicted ANN model, Root Mean Square error (RMSE) was

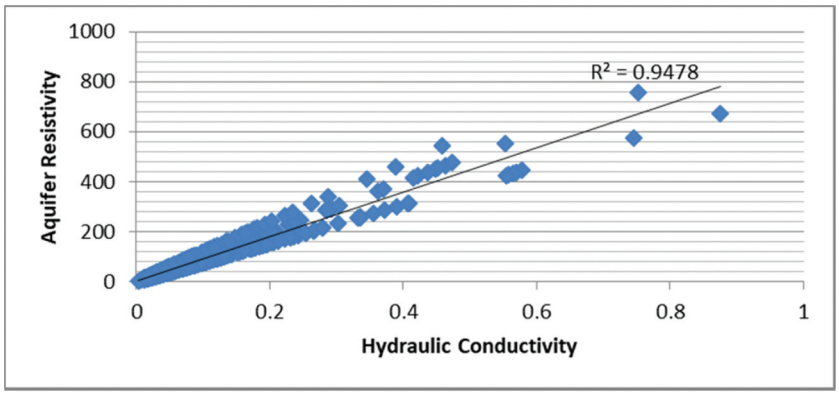

Figure 14. Correlation plot between aquifer resistivity and hydraulic conductivity.

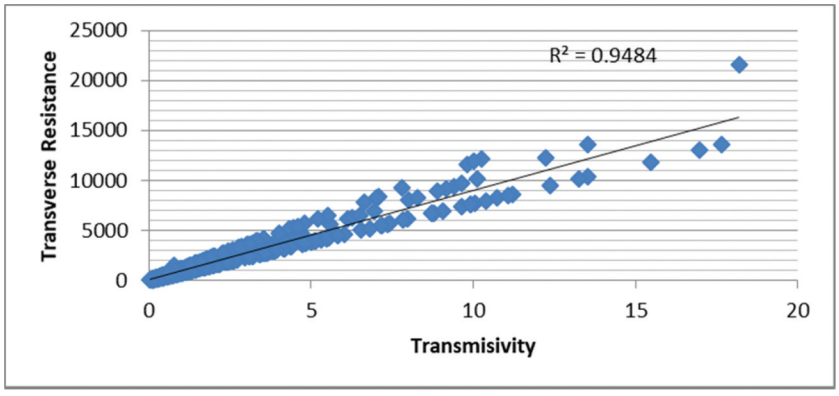

Figure 15. Corelation plot between transverse resistance and transmisivity.

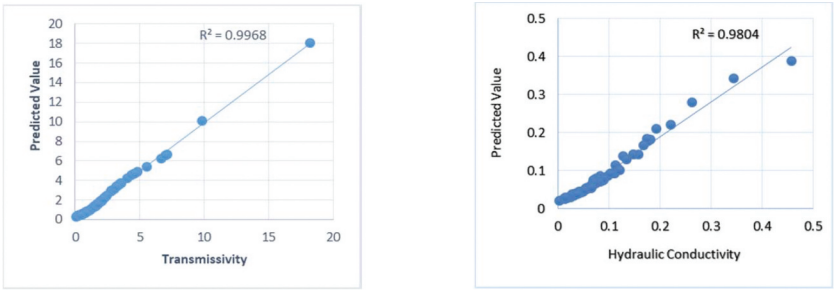

Figure 16. Regression plot for the training of the ANN model generated for the prediction of (a) Transmissivity (b) Hydraulic conductivity on Quartzite/Quartz Schist Lithology.

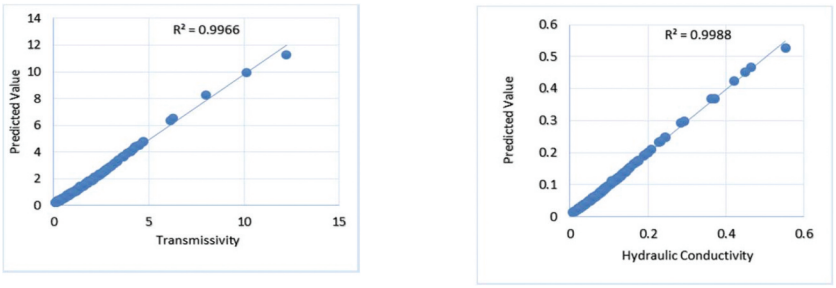

Figure 17. Regression plot for the training of the ANN model generated for the prediction of (a) Transmissivity (b) Hydraulic conductivity on Undifferentiated Schist Lithology.

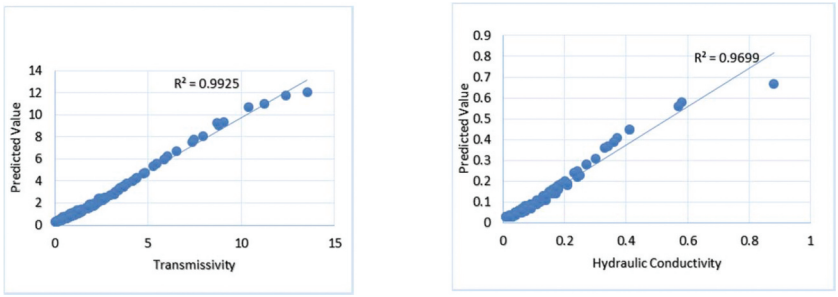

Figure 18. Regression plot for the training of the ANN model generated for the prediction of (a) Transmissivity (b) Hydraulic conductivity on migmatite lithology.

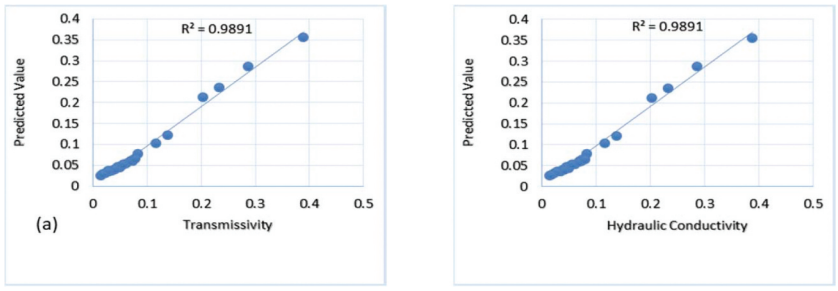

Figure 19. Regression plot for the testing of the ANN model generated for the prediction of (a) Transmissivity (b) Hydraulic conductivity on quartzite/quartz schist lithology.

calculated. The calculated RMSE for the model show values ranging from 0.063 to 0.250. The low-value of RMSE values (Table 3) indicated high predictive performances of the model.

4. Conclusions

A combined geophysical, hydrogeological, and statistical modelling approach has been used to predict hydraulic conductivity and transmissivity within Ibadan

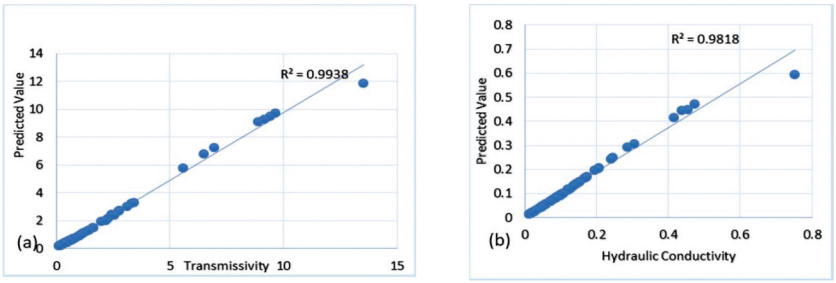

Figure 20. Regression plot for the testing of the ANN model generated for the prediction of (a) Transmissivity on (b) Hydraulic conductivity undifferentiated schist lithology.

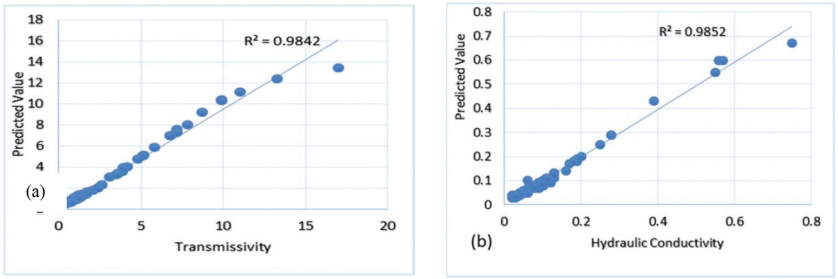

Figure 21. Regression plot for the testing of the ANN model generated for the prediction of (a) Transmissivity (b) Hydraulic conductivity on migmatite lithology.

Table 3. RMSE values for the proposed model.

Rock Type	RMSE Value for T	RMSE Value for K
Quartzite/Quartz-Schist	0.09	0.250
Undifferentiated Schist	0.063	0.079
Migmatite Gneiss	0.207	0.076
The Whole Study Area	0.098	0.087

Metropolis, south-western Nigeria. Dar-Zarrouk parameter which is a secondary derivative of geo-electric data has proven to be a useful tool in estimating hydraulic parameters. The good correlation (r = 0.95) between transverse resistance R (Ωm^2) and transmissivity further confirms the established relationship between hydraulic and Dar-Zarrouk parameters. ANN has been used in this study to predict transmissivity and hydraulic conductivity from geo-electric data in south-western Nigeria's basement complex area. The measurement of the degree of uncertainty reveals that in predicting T and K, the Artificial Neural Network model generated is reliable. The degree of correlation between the observed and predicted values of T and K ranges from 0.97 to 0.99. In addition, the ANN model's RMSE value was found to be within 0.063–0.250 suggesting the model's high performance. Nevertheless, it is worth noting that the expected derived equation is applicable only for aquifers with similar characteristics or geology that have been studied.

Disclosure statement

No potential conflict of interest was reported by the authors.

ORCID

M. A. Oladunjoye http://orcid.org/0000-0002-6162-4170
M. A. Adeniran http://orcid.org/0000-0002-4889-9655

References

Ahmed S, Marsily GD, Talbot A. 1988. Combined use of hydraulic and electrical properties of an aquifer in a geo-statistical estimation of transmissivity. Ground Water Hydrol. 26(1):78–86.

Al-Sulaiman MA, Aboukarima AM. 2016. Prediction of unsaturated hydraulic conductivity of agricultural soils using artificial neural network and C#. J Agric Ecol Res Int. 5(4):1–15. doi:10.9734/JAERI/2016/21622.

Bart R, Dirk M, Okke B, Matej G, Marijke H, Alain D. 2016. Estimation of hydraulic conductivity and its uncertainty from grain-size data using GLUE and artificial neural networks. Int Assoc Math Geosci. 44:739–763.

Basheer IA, Hajmeer M. 2000. Artificial neural networks: fundamentals computing design and application. J Microbiol Methods. 43(1):3–31. doi:10.1016/S0167-7012(00)00201-3.

Giansilvio P, Arcadio O, Mauro M. 1984. Empirical relationship between electrical transverse resistance and hydraulic transmissivity. Geoexploration. 22(1):1–15. doi:10.1016/0016-7142(84)90002-4.

Halford KJ, Kuniasky EL. 2002. Documentation of spreadsheet for the analysis of aquifer test and slug test data. U. S. Geological Survey Open-File Report 02-197; p. 54.

Hornik K, Stinchcombe M, White H. 1989. Multilayer feed-forward networks are universal approximators. Neural Network. 2(5):359–366. doi:10.1016/0893-6080(89)90020-8.

Jones HA, Hockey RD. 1964. The geology of part of south-western Nigeria. Geol Survey Niger Bull. 31:101.

Kumar MS, Gnanasundar D, Elango L. 2001. Geological studies to determine hydraulic characteristics of an alluvial aquifer. J Environ Hydrol. 9:1–8. Paper 15.

Maillet R. 1947. The fundamental equations of electrical prospecting. J Geophys. 12:527–556.

Murali S, Patangay NS. 2006. Principles of application of groundwater geophysics. In: Association of geophysicsists. 3rd ed. Hyderbad, India: Association of Exploration Geophysicists. p. 371.

Niwas S, Lima OAL. 2003. Aquifer parameter estimation from surface resistivity data. Ground Water. 41(1):95–99. doi:10.1111/j.1745-6584.2003.tb02572.x.

Niwas S, Singhal DC. 1981. Estimation of aquifer transmissivity from Dar- Zarrouk parameters in porous media. J Hydrol. 50:393–399. doi:10.1016/0022-1694(81)90082-2.

Nur A, Goji M. 2005. Hydro-geoelectric study in Takum and environs of Taraba State. NE. Niger Global J Geol Sci. 3(2):393–399.

Oladunjoye MA, Jekayinfa S. 2015. Efficacy of Hummel (Modified Schlumberger) arrays of vertical electrical sounding in groundwater exploration: case study of parts of | Ibadan Metropolis, Southwestern Nigeria. Int J Geophys. 2015:24. Id. 162303. doi:10.1155/2015/612303.

Reiter PF. 1981. A computer study of the correlation between aquifer hydraulic and electrical properties [Thesis presented to the University of Rhode Island at Kingstone R. I, in partial fulfilment of the requirement for the degree of Master of Science].

Sanuade OA, Oyeyemi K, Amosun JO, Fatoba J. 2018. Prediction of transmissivity of aquifer from geo-electric data using artificial neural network. IOP Conf Ser Earth Environ Sci. 173:012025. doi:10.1088/1755-1315/173/1/012025.

Singh UK, Tiwari R, Singh S. 2013. Neural network modelling and prediction of resistivity structures using VES Schlumberger data over a geothermal area. J Comput Geosci. 52:246–257. doi:10.1016/j.cageo.2012.09.018.

Soupios PM, Kouli M, Vallianatos F, Vafidis A, Stavroulakis G. 2007. Estimation of aquifer hydraulic parameters from surficial geophysical methods: a case study of Keritis Basin in Chania (Crete-Greece). J Hydrol. 338(1–2):122–131. doi:10.1016/j.jhydrol.2007.02.028.

Tijani MN, Alichi UA, Diop S. 2009. Impact of Bedrock types on the hydraulic characteristic of weathered basement aquifers; A case study from Southwestern Nigeria. Joint International Convention of 8th IAHS Scientific Assembly and 37th IAH Congress; Hyderabad, India.

Tijani MN, Oluchukwu IN, Oladunjoye MA. 2018. Estimation of hydraulic properties from resistivity sounding data: a case study of basement aquifer in Ibadan, SW – Nigeria. J Min Geol. 54(I):59–74.

Ungemach P, Mostaghimi F, Duprat A. 1969. Tests for determination of storage coefficient in unconfined aquifer and application in alluvial aquifer of Rhin. Bull Int Assoc Sci Hydrol. 14(2):169–190. doi:10.1080/02626666909493726.

Youssef MAS. 2020. Geoelectrical analysis for evaluating the aquifer hydraulic characteristics in Ain El-Soukhna Area, West Gulf of Suez, Egypt. NRIAG J Astron Geophys. 9(1):85–98. doi:10.1080/20909977.2020.1713583.